

The multiple phenylpropene synthases in both *Clarkia breweri* and *Petunia hybrida* represent two distinct protein lineages

Takao Koeduka¹, Gordon V. Louie², Irina Orlova³, Christine M. Kish³, Mwafaq Ibdah¹, Curtis G. Wilkerson⁴, Marianne E. Bowman², Thomas J. Baiga², Joseph P. Noel², Natalia Dudareva³ and Eran Pichersky^{1,*}

¹Department of Molecular, Cellular and Developmental Biology, University of Michigan, 830 North University Street, Ann Arbor, MI 48109-1048, USA,

²Howard Hughes Medical Institute, Jack H. Skirball Center for Chemical Biology and Proteomics, The Salk Institute for Biological Studies, 10010 N. Torrey Pines Road, La Jolla, CA 92037, USA,

³Department of Horticulture and Landscape Architecture, Purdue University, West Lafayette, IN 47907, USA, and

⁴Department of Energy Plant Research Laboratory and Michigan Proteome Consortium, Michigan State University, East Lansing, MI 48824, USA

Received 13 November 2007; revised 19 December 2007; accepted 21 December 2007.

*For correspondence (fax +1 734 647 0884; e-mail lel@umich.edu).

Summary

Many plants synthesize the volatile phenylpropene compounds eugenol and isoeugenol to serve in defense against herbivores and pathogens and to attract pollinators. *Clarkia breweri* flowers emit a mixture of eugenol and isoeugenol, while *Petunia hybrida* flowers emit mostly isoeugenol with small amounts of eugenol. We recently reported the identification of a petunia enzyme, isoeugenol synthase 1 (PhIGS1) that catalyzes the formation of isoeugenol, and an *Ocimum basilicum* (basil) enzyme, eugenol synthase 1 (ObEGS1), that produces eugenol. ObEGS1 and PhIGS1 both utilize coniferyl acetate, are 52% sequence identical, and belong to a family of NADPH-dependent reductases involved in secondary metabolism. Here we show that *C. breweri* flowers have two closely related proteins (96% identity), CbIGS1 and CbEGS1, that are similar to ObEGS1 (58% and 59% identity, respectively) and catalyze the formation of isoeugenol and eugenol, respectively. *In vitro* mutagenesis experiments demonstrate that substitution of only a single residue can substantially affect the product specificity of these enzymes. A third *C. breweri* enzyme identified, CbEGS2, also catalyzes the formation of eugenol from coniferyl acetate and is only 46% identical to CbIGS1 and CbEGS1 but more similar (>70%) to other types of reductases. We also found that petunia flowers contain an enzyme, PhEGS1, that is highly similar to CbEGS2 (82% identity) and that converts coniferyl acetate to eugenol. Our results indicate that plant enzymes with EGS and IGS activities have arisen multiple times and in different protein lineages.

Keywords: secondary metabolism, biochemistry, protein structure, plant volatile, scent.

Introduction

Eugenol and isoeugenol belong to a class of compounds, the phenylpropenes, which are derived from phenylalanine. The phenylpropenes are important constituents in many spices used by humans and have therefore played important roles in human nutrition (Prasad *et al.*, 2004). The phenylpropenes are generally toxic to animals and microorganisms, and many plants synthesize them in their vegetative parts as defense against herbivores and

pathogens (Grossman, 1993; Obeng-Ofori and Reichmuth, 1997).

The floral scent bouquet of many species contains volatile phenylpropenes. For example, the flowers of the California annual *Clarkia breweri* emit a mixture of volatiles that include eugenol, isoeugenol, methyleugenol, and methylisoeugenol (Raguso and Pichersky, 1995; Figure 1a). Flowers of *Petunia hybrida*, another moth-pollinated species, emit

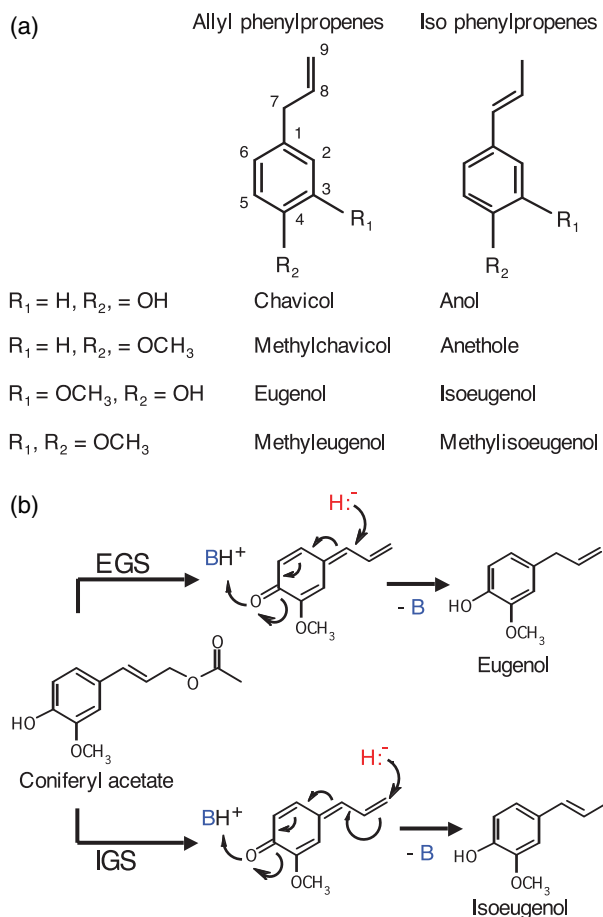


Figure 1. Structures of representative phenylpropenes and proposed reaction mechanism of eugenol synthase (EGS) and isoeugenol synthase (IGS). (a) Structures of chavicol, anol, eugenol, isoeugenol, and their methylated derivatives. The carbon numbering system used in the text is shown. (b) The proposed reaction mechanism of EGS and IGS uses a quinone-methide intermediate (Louie *et al.*, 2007). B (in blue) represents a general base consisting of K132 and a bridging water molecule. H^- (in red) represents the hydride transferred from NADPH.

high levels of isoeugenol, as well as smaller amounts of eugenol (Verdonk *et al.*, 2003). Many herbs, such as basil, also synthesize and store phenylpropenes in glands on their leaves (Gang *et al.*, 2001).

We have recently shown that petunia flowers possess a NADPH-dependent enzyme, isoeugenol synthase 1 (PhIGS1), which converts coniferyl acetate to isoeugenol, while leaf glands of basil (*Ocimum basilicum*) possess the enzyme eugenol synthase 1 (ObEGS1), which converts the same precursor to eugenol (Koeduka *et al.*, 2006). The PhIGS1 and ObEGS1 proteins are approximately 50% identical and are also homologous to several other reductases involved in phenylpropanoid metabolism in plants, including pinoreisnol-lariciresinol reductase (PLR), isoflavone reductase (IFR), phenylcoumaran benzylic ether reductase (PCBER), leucocyanidin reductase (LAR), and pterocarpan reductase (PTR),

collectively termed the PIP reductase family after the first three enzymes discovered in this family (Akashi *et al.*, 2006; Gang *et al.*, 1999; Min *et al.*, 2003; Tanner *et al.*, 2003).

Eugenol and isoeugenol differ in the position of the double bond in the propene side chain (Figure 1a). PhIGS1 and ObEGS1 represent an interesting example of two similar enzymes that use the same substrate but catalyze the formation of a different product. Recently, the crystal structure of ObEGS1 complexed with $NADP^+$ and a coniferyl-acetate analog was obtained (Louie *et al.*, 2007). Examination of this structure shows that the enzyme acts on the substrate via a 'push-pull' mechanism, removing the proton of the *para*-hydroxyl group and promoting the cleavage of the acetyl group. In the resultant quinone-methide intermediate, the C7 atom serves as the acceptor of the hydride ion from NADPH (Figure 1b). Presumably, the position of the substrate in the active site of PhIGS1 is such that the hydride is transferred to C9 instead of C7 (Figure 1b). However, the high overall level of divergence between the two enzymes precludes an easy identification of the residues involved without additional structural information, and attempts to crystallize PhIGS1 have so far failed.

Because *C. breweri* flowers, unlike petunia flowers or basil glands, emit a mixture of both eugenol and isoeugenol in roughly similar proportions, we investigated whether a single enzyme is responsible for their biosynthesis, or, if two or more enzymes are involved, how related they are to each other and to PhIGS1 and ObEGS1. Our results indicate that *C. breweri* flowers have a eugenol synthase and an isoeugenol synthase (CbEGS1 and CbIGS1) that are closely related to each other, and that the differing product specificity is determined by very few residues. Furthermore, *C. breweri* possesses a second eugenol synthase (CbEGS2) that is very unlike both CbEGS1 and CbIGS1 and is more related to non-phenylpropene producing enzymes. We also discovered that petunia has a eugenol synthase that is closely related to CbEGS2. These results suggest that both convergent and divergent evolutionary pathways have given rise to phenylpropene-forming enzymes in plants.

Results

Levels of eugenol synthase and isoeugenol synthase activities in C. breweri

Enzyme activity measurements from crude protein extracts obtained from different floral parts 1 day post-anthesis indicated that the highest levels of IGS-specific activity were found in petals, followed by stamens, pistil, and sepals, with no activity in leaves (Table 1). The highest specific activity levels of EGS were found in the stamens, followed closely by the pistil and petals (Table 1). However, since the petal tissue constitutes the bulk of the flower (Pichersky *et al.*, 1994), the highest overall amounts of enzymatic activities for both

Table 1 Isoeugenol synthase (IGS) and eugenol synthase (EGS) activities from crude extracts of different parts of *Clarkia breweri* flowers at 1 day post-anthesis

Organ (total WT per flower)	IGS		EGS	
	Specific activity (pkat g FW ⁻¹)	Total activity (pkat flower ⁻¹)	Specific activity (pkat g FW ⁻¹)	Total activity (pkat flower ⁻¹)
Leaves	ND	ND	ND	ND
Sepals (22.5 mg)	0.03 ± 0.00	0.65 ± 0.09	0.03 ± 0.01	0.72 ± 0.11
Petals (64 mg)	0.32 ± 0.04	20.74 ± 2.37	0.05 ± 0.00	3.07 ± 0.13
Stamens (24 mg)	0.13 ± 0.03	3.22 ± 0.60	0.06 ± 0.01	1.54 ± 0.14
Pistil (16 mg)	0.05 ± 0.01	0.72 ± 0.18	0.05 ± 0.01	0.86 ± 0.10

Values are the averages of three independent experiments ± SE. FW, fresh weight; ND, not detected; WT, wild type.

EGS and IGS occur in the petals (Table 1). These results are consistent with previous observations that emission of eugenol, isoeugenol, and their methylated derivatives from *C. breweri* flowers occurred mostly from petals (Wang *et al.*, 1997).

Purification of EGS and IGS activities from petals of *C. breweri*

Both IGS and EGS activities were therefore purified from petals in a protocol employing several chromatographic steps (Table 2). Fractions were monitored for both IGS and EGS activities. After diethylaminoethyl (DEAE) chromatography, a broad peak with both IGS and EGS activities was obtained. Two separate peaks of EGS activity were observed eluting from the Hitrap-Phenyl column, while only a single peak of IGS activity was obtained from this column, co-eluting with the earlier peak of EGS activity (EGS peak 1 described in Table 2). The fractions of peak 1

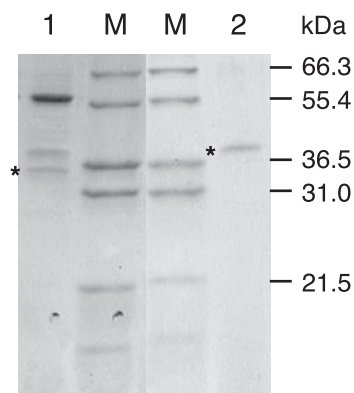


Figure 2. A composite SDS-PAGE gel showing purified isoeugenol (IGS) and eugenol (EGS) synthases from *Clarkia breweri* petals. Lane 1, An aliquot of the fraction with peak IGS and EGS activities from Hitrap-Q column 1 (aliquot contains 0.94 pkat IGS activity). Lane 2, An aliquot of the fraction with peak EGS activity from Hitrap-Q column 2 (0.81 pkat EGS activity). M, marker lanes (molecular weights indicated on the right). The gels were stained with Coomassie Blue after SDS-PAGE electrophoresis. The bands corresponding to CbEGS1/CbIGS1 (lane 1) and CbEGS2 (lane 2) are marked with asterisks.

were pooled and loaded on a Hitrap-Q column, and eluted with a KCl gradient. The IGS and EGS activities eluting from this column did not separate, and the fractions in the peak of IGS and EGS activities contained three major bands of approximately 55, 38, and 36 kDa (Figure 2, lane 1). The presence of the 36-kDa protein (marked with an asterisk in Figure 2, lane 1) correlated best with IGS and EGS activities in the various fractions. The fractions containing EGS activity in peak 2 of the Hitrap-Phenyl column were also pooled and loaded onto a second Hitrap-Q column, and activity was eluted with a KCl gradient. A sharp peak of EGS activity was obtained (150–230 mM KCl range), and the pooled fractions of this peak contained a single protein of approximately 38 kDa (marked with an asterisk in Figure 2, lane 2) with EGS activity.

Table 2 Purification of isoeugenol synthase (IGS) and eugenol synthase (EGS) from *Clarkia breweri* petals

Purification step	Total protein (mg)	Total activity (pkat)		Specific activity (pkat mg ⁻¹)		Purification (-fold)		Recovery (%)	
		IGS	EGS	IGS	EGS	IGS	EGS	IGS	EGS
Crude extract	344.0	1448.1	367.5	4.2	1.1	1.0	1.0	100.0	100.0
DE-53	98.6	671.4	330.3	6.8	3.4	1.6	3.1	46.4	89.9
Hitrap-Phenyl (peak 1) ^a	18.8	110.5	110.4	5.9	5.9	1.4	5.4	7.6	30.0
Hitrap-Phenyl (peak 2) ^a	3.1	–	158.0	–	50.6	–	46.0	–	43.0
Hitrap-Q col. 1	3.6	139.6	107.4	38.8	29.8	9.2	27.1	9.6	29.2
Hitrap-Q col. 2	0.9	–	108.1	–	118.8	–	108.0	–	29.4

^aThere were two peaks of EGS activities eluting from the Hitrap-Phenyl column, and the single peak of IGS activity coincided with the first peak of EGS activity on this column, as described in the text. Data in this table labeled peak 1 and peak 2 were obtained from pooled fractions constituting each peak.

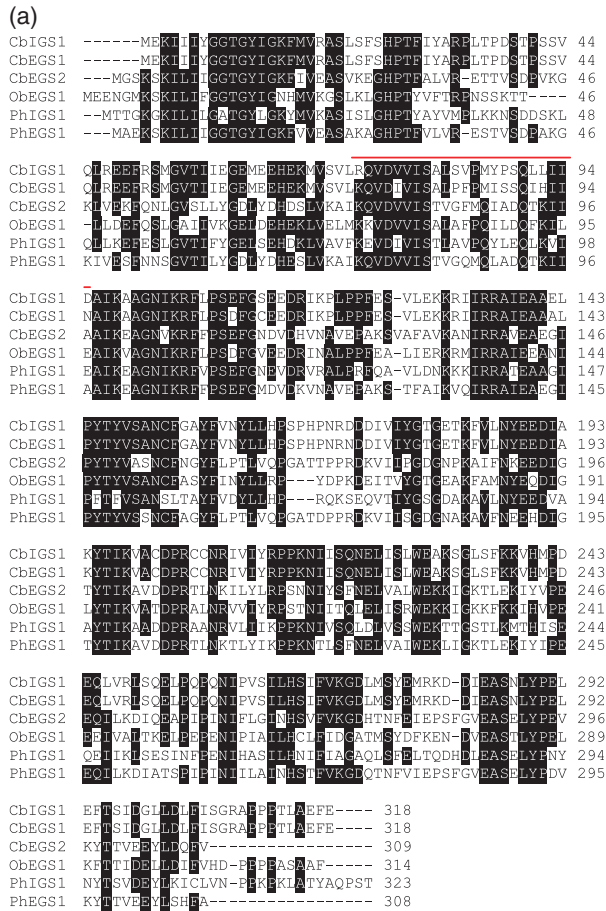
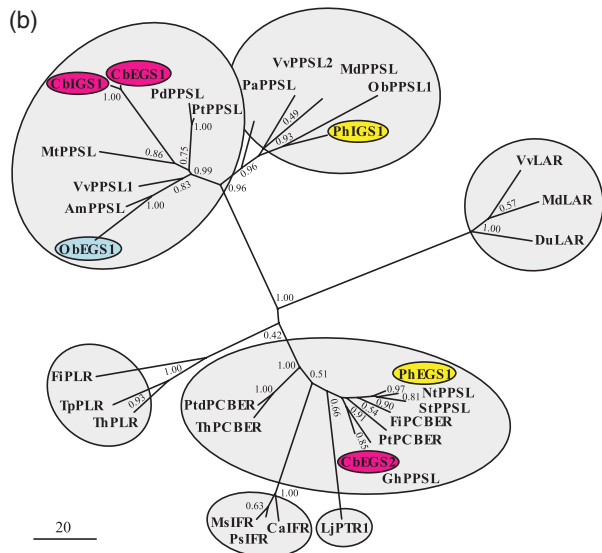


Figure 3. Sequence comparisons of CbIGS1, CbEGS1, CbEGS2, and representative PIP proteins.

(a) A comparison of amino acid sequences of *Clarkia breweri* CbIGS1, CbEGS1, and CbEGS2, petunia PhIGS1 and PhEGS1, and basil ObEGS1. White letters on black background represent identical residues in at least four sequences. The region highly divergent between CbEGS1 and CbIGS1 (positions 73–95) is indicated by a red line.

(b) Phylogenetic analysis of selected protein sequences in the PIP family showing an unrooted maximum likelihood tree. The scale indicates the number of substitutions per site. In addition to isoegenol synthase (IGS)/eugenol synthase (EGS)-like proteins, the PIP family includes pinoresinol-lariciresinol reductases (PLR), isoflavone reductases (IFR), phenylcoumaran benzylic ether reductases (PCBER), leucocyanidin reductase (LAR), and pterocarpan reductase (PTR). Proteins biochemically characterized in *C. breweri*, basil, and petunia are shown on a red, blue, and yellow background, respectively. Proteins for which no specific activity has been assigned are designated here as PPSL (phenylpropane synthase-like). The position of the PLR branch is uncertain (bootstrap value of 0.42), and in the neighbor-joining and maximum parsimony trees (not shown) it is closer to the ObEGS1/PhIGS1 clades. The only other disagreement among the three trees – the positions of the IFR branch and the PTR branch, which is also uncertain in the maximum likelihood tree – is discussed in the text. Am, *Antirrhinum majus*; Ca, *Cicer arietinum*; Cb, *Clarkia breweri*; Du, *Desmodium uncinatum*; Fi, *Forsythia intermedia*; Gh, *Gossypium hirsutum*; Lj, *Lotus japonica*; Md, *Malus domestica*; Ms, *Medicago sativa*; Mt, *Medicago truncatula*; Nt, *Nicotiana tabacum*; Ob, *Ocimum basilicum*; Pa, *Persea americana*; Pd, *Populus deltoides*; Ph, *Petunia hybrida*; Ps, *Pisum sativum*; Pt, *Populus trichocarpa*; Ptd, *Pinus taeda*; St, *Solanum tuberosum*; Th, *Tsuga heterophylla*; Tp, *Thuja plicata*; Vv, *Vitis vinifera*. The accession numbers of the proteins are given in Table S2.



Isolation and characterization of *C. breweri* cDNAs encoding proteins with IGS and EGS activities

The 36-kDa protein band obtained in the final purification step (HiTrap-Q column) from the peak of mixed EGS/IGS activity originally obtained from the HiTrap-Phenyl

column (Figure 2, lane 1) was eluted from the gel, trypsinized, and sequenced by liquid chromatography-tandem mass spectrometry (LC-MS/MS), followed by screening a *C. breweri* flower expressed sequence tag (EST) database comprising around 2000 sequences (D’Auria *et al.*, 2002). The seven peptide sequences obtained from this 36-kDa protein band were found in the predicted protein sequences encoded by two closely related EST that fell into two contigs, and there were no other sequences encoding any of these peptides. Because of the short nature of the sequences in this database (<500 nucleotides) and the few differences between the two contigs, it was not possible to unambiguously assign all seven ESTs to one contig or the other. However, there was one region that was clearly different between the two contigs (Figure 3a), although none of the seven peptide sequences obtained corresponded to this region. We subsequently designated the two genes represented by these two contigs as *CbEGS1* and *CbIGS1*. Based on comparisons with ObEGS1 and PhIGS1, the contig representing *CbEGS1* contained a complete open reading frame, but the contig representing *CbIGS1* was missing the 5’ end. A rapid amplification of 5’ complementary DNA ends (5’ RACE) experiment was conducted to obtain the sequence of the beginning of *CbIGS1*, using an internal primer based on sequence in a divergent region between *CbEGS1* and *CbIGS1* (Table S1). The sequence thus obtained showed that the nucleotide sequences of *CbEGS1* and *CbIGS1* around the beginning of the open reading frame were identical to each other. Based on this information, additional cDNAs (>10) of

CbEGS1 and *CbIGS1* were generated by RT-PCR with primers designed for the beginning and end of the open reading frame, and the sequences of all cDNAs thus obtained were identical to either *CbEGS1* or *CbIGS1*.

The single protein with an approximate molecular mass of 38 kDa present in the fractions constituting the peak EGS activity eluting from the second Hitrap-Q column (Figure 2, lane 2) was analyzed in the same way. The sequence of 11 peptides obtained from it matched the sequence of a protein encoded by a gene represented by four ESTs in the database constituting a single contig that was deemed to contain the entire coding region (based on comparison with PCBER proteins, see below). We consequently designated this gene as *CbEGS2* and the protein it encodes as CbEGS2 (Figure 3a). There were no other EST variants encoding any of these peptides.

Transcript levels of *CbEGS1*, *CbIGS1*, and *CbEGS2* were measured and found to be highest in petals; no transcripts were found in leaves (Figure 4a). Both *CbEGS1* and *CbIGS1* encode proteins of 318 amino acids (aa) with a calculated molecular mass of 36.0 kDa. When *CbIGS1* and *CbEGS1* were expressed in *Escherichia coli*, the resulting (non-His-tagged) proteins co-migrated on SDS-PAGE with the 36 kDa protein from Figure 2, lane 1 (data not shown). *CbEGS2* encodes a protein of 309 amino acids with a calculated molecular mass of 34.2 kDa. Expression of full-length, non-fusion cDNA of *CbEGS2* in *E. coli* resulted in a protein co-migrating with the 38 kDa from Figure 2, lane 2 (data not shown). These results indicate that the characterized cDNAs of *CbEGS1*, *CbIGS1*, and *CbEGS2* each contain the complete coding information for the respective proteins.

The full-length cDNAs of *CbEGS1*, *CbIGS1*, and *CbEGS2* were expressed in *E. coli* to produce His-tagged CbEGS1, CbIGS1, and CbEGS2 proteins, which were then purified and assayed for activity with coniferyl acetate. The purified CbIGS1 enzyme catalyzed the formation of only isoeugenol (Figure 5a). The purified CbEGS1 and CbEGS2 proteins produced only eugenol (Figure 5b,c, respectively).

Analysis of the evolutionary relatedness of *CbEGS1*, *CbIGS1* and *CbEGS2* to each other and to other PIP proteins

The CbEGS1 and CbIGS1 proteins are 95.9% identical to each other. A phylogenetic analysis based on the maximum likelihood method (Figure 3b) as well as other methods including neighbor-joining and maximum parsimony (not shown) all indicated that CbEGS1 and CbIGS1 are the most closely related, among biochemically characterized proteins, to ObEGS1 (52% identity) as well as to PhIGS1 (51% identity; Figure 3b). CbEGS2, however, is more closely related to several enzymes previously characterized (Gang *et al.*, 1999) to have PCBER activity (Figure 3b). For example, it is 78% identical to *Populus trichocarpa* PCBER, but only 46% identical to CbEGS1 or CbIGS1.

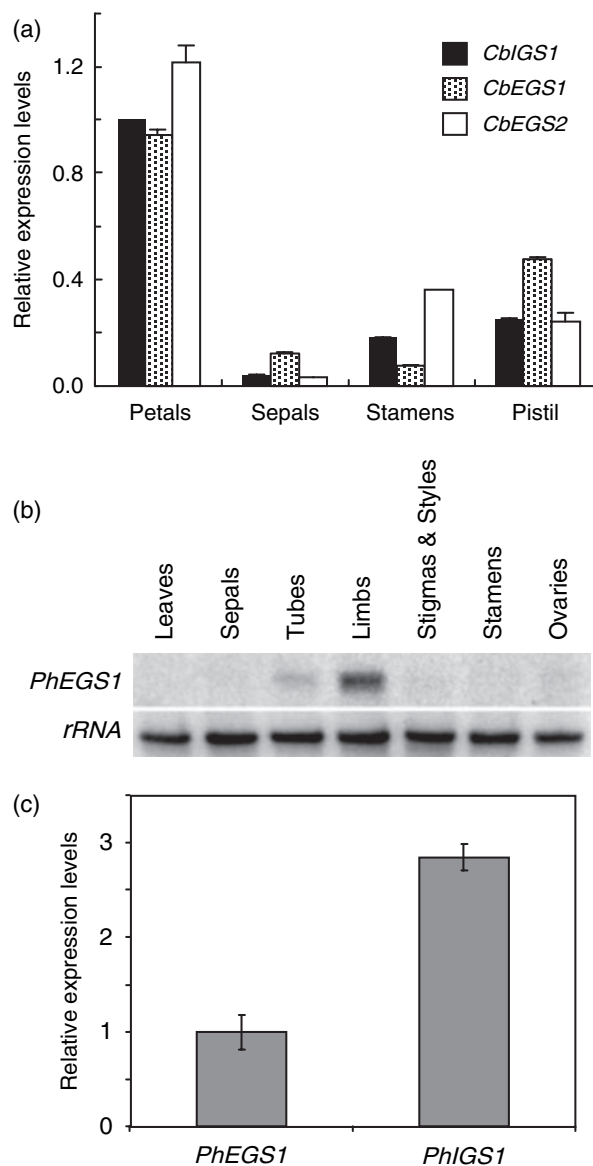


Figure 4. Detection of *CbIGS1*, *CbEGS1*, *CbEGS2*, *PhIGS1*, and *PhEGS1* transcripts in different organs by qRT-PCR and northern blot.

(a) *CbIGS1*, *CbEGS1*, and *CbEGS2* transcript levels from different floral organs at 1 day pre-anthesis (when the mRNA levels of these genes are highest). Each graph represents the average of three replications for two independent experiments using two biological samples. Bars indicate SE.

(b) Tissue specificity of *PhEGS1* mRNA. Shown is a representative RNA gel blot of total RNA (5 μ g per lane), isolated from leaves and different organs of 2-day-old petunia flowers, probed with *PhEGS1* (top). The blot was rehybridized with an 18S rDNA probe (bottom) to ascertain equal loading of RNA.

(c) The relative *PhIGS1* and *PhEGS1* mRNA levels in corollas of 2-day-old petunia flowers as determined by qRT-PCR. *PhEGS1* expression was set as 1. Bars indicate SE.

Isolation of a petunia eugenol synthase 1 (*PhEGS1*) closely related to *CbEGS2*

Since petunia flowers emit small amounts of eugenol in addition to high levels of isoeugenol (eugenol levels are <3%

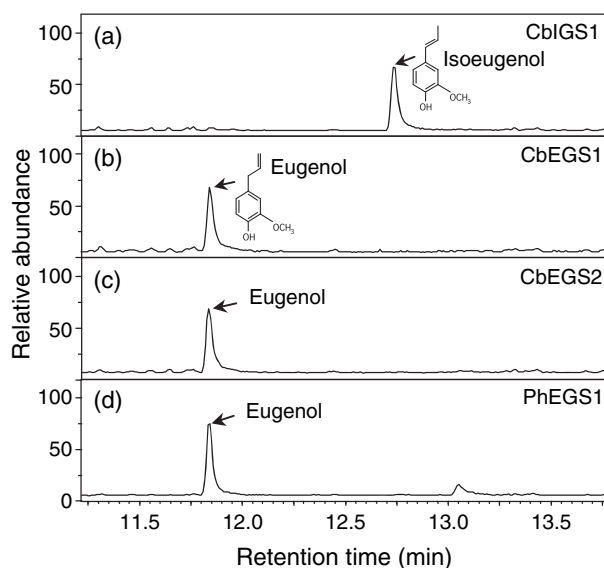


Figure 5. Product analysis of reactions catalyzed by CbIGS1, CbEGS1, CbEGS2, and PhEGS1 using coniferyl acetate as substrate.

Enzyme assays contained 0.5 mM coniferyl acetate, 1 mM NADPH, and 1 μ g purified enzymes, and were incubated for 30 min at RT. Reaction products were analyzed by gas chromatography/mass spectrometry. Relative abundance is shown in arbitrary units, based on total ion current measurement.

- (a) Reaction catalyzed by *Clarkia breweri* IGS1.
 (b) Reaction catalyzed by *C. breweri* EGS1.
 (c) Reaction catalyzed by *C. breweri* EGS2.
 (d) Reaction catalyzed by *petunia* EGS1.

of those of isoeugenol, Verdonk *et al.*, 2003), and the previously characterized PhIGS1 catalyzes the formation of isoeugenol but not eugenol, the origin of eugenol in *petunia* was not clear. A search of *petunia* flower EST databases (containing >3000 ESTs) identified several cDNAs encoding a protein of 308 aa with 82.1% identity to CbEGS2 (Figure 3), but no other cDNAs encoding proteins with similarity to known IGS and EGS sequences. This 308-aa protein, designated as *Petunia hybrida* eugenol synthase 1 (PhEGS1), has only 47.7% aa identity to PhIGS1. Characterization of purified PhEGS1 produced in *E. coli* revealed that the protein catalyzes the formation of eugenol from coniferyl acetate (Figure 5d). *PhEGS1* is expressed specifically in the scent-producing parts of the flowers (limbs and tube) but not in other parts of the flowers nor in leaves (Figure 4b). *PhEGS1* transcript levels were about threefold lower than those of *PhIGS1* (Figure 4c).

Enzymatic properties of *C. breweri* IGS1, EGS1, and EGS2 and *P. hybrida* EGS1

The apparent K_m values of CbIGS1, CbEGS1, and CbEGS2 for coniferyl acetate were 212 ± 28 , 93 ± 6 , and 311 ± 45 μ M, respectively (Table 3). The apparent k_{cat} value of CbIGS1 was 0.99 ± 0.13 sec^{-1} and the corresponding values for CbEGS1 and CbEGS2 were 0.26 ± 0.01 and

Table 3 Kinetic parameters of *Clarkia breweri* and *Petunia hybrida* eugenol synthase (EGS) and isoeugenol synthase (IGS) enzymes for coniferyl acetate

Enzymes	K_m (μ M)	V_{max} (nmol sec^{-1} mg^{-1})	k_{cat} (sec^{-1})	k_{cat}/K_m (sec^{-1} mM^{-1})
CbIGS1	211.5 ± 27.9	27.6 ± 3.7	0.99 ± 0.13	4.7
CbEGS1	93.3 ± 6.3	7.3 ± 0.2	0.26 ± 0.01	2.8
CbEGS2	310.5 ± 45.2	6.9 ± 0.6	0.25 ± 0.02	0.8
PhEGS1	245.3 ± 58.0	18.4 ± 1.6	0.60 ± 0.05	2.4
PhIGS1	226.1 ± 70.3	35.7 ± 5.9	1.3 ± 0.2	5.7

Values are averages of three independent experiments \pm SE.

0.25 ± 0.02 sec^{-1} . Thus, the apparent catalytic efficiency (k_{cat}/K_m) of CbIGS1 is about twofold higher than CbEGS1 and six-fold higher than that of CbEGS2 (Table 3). PhEGS1 has a K_m value for coniferyl acetate of 245 μ M and a k_{cat} of 0.60 sec^{-1} , similar to the re-measured K_m value for PhIGS1, but its turnover rate is twofold lower than that of PhIGS1 (Table 3).

Because of the sequence similarity of CbEGS2 and PhEGS1 to proteins characterized as PCBER enzymes, we tested them as well as CbEGS1, CbIGS1, and the previously characterized ObEGS1 and PhIGS1 (Koeduka *et al.*, 2006) for their ability to reduce the PCBER substrate dehydroconiferyl alcohol (DDC) to isodihydrodehydroconiferyl alcohol (IDDDC). No IDDDC product was detected in any of these reaction assays after 1 h. (In the control assays containing coniferyl acetate instead of DDC with the same amount of protein and carried out for 1 h, >35% of the substrate was converted to the product.) When the enzymatic assays using DDC as a substrate were carried out over longer time periods (>3 h) and with a 23-fold increase in protein concentration, ObEGS1, PhIGS1, CbIGS1, and CbEGS1 were still not able to reduce any DDC to IDDDC (Figure 6a–d); however, CbEGS2 and PhEGS1 catalyzed the formation of a small amount of IDDDC (Figure 6e,f) at the calculated rates of 6.7 and 24.4 nmol h^{-1} (mg protein^{-1}) $^{-1}$, respectively. These rates were comparable to the rates of 53 and 104.2 nmol h^{-1} (mg protein^{-1}) $^{-1}$ reported for *P. trichocarpa* and *Pinus taeda* PCBERs, respectively (Gang *et al.*, 1999), but are approximately 2700- to 4000-fold slower than the rates in which PhEGS1 and CbEGS2, respectively, catalyze the production of eugenol from coniferyl acetate (Table 3).

Amino acid residues in CbIGS1, CbEGS1, and other EGS and IGS proteins involved in determining product specificity

Sequence comparison of CbIGS1 and CbEGS1 show that they differ at only 13 positions, and nine of these positions reside in a small region between positions 73 and 95 (Figure 7). To identify the specific residues that determine their product specificity, we first produced a hybrid protein

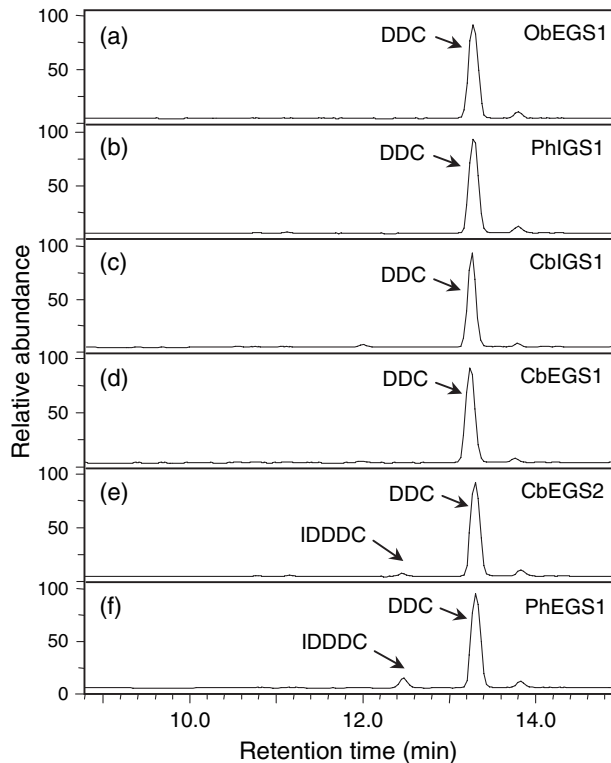


Figure 6. Product analyses of reactions catalyzed by CbIGS1, CbEGS1, CbEGS2, PhEGS1, PhIGS1, and ObEGS1, using dehydrodihydroconiferyl alcohol (DDC) as substrate. Enzyme assays contained 0.5 mM DDC, 1 mM NADPH, and 22.5 μ g purified enzymes, and were incubated for 19 h. Reaction products were analyzed by liquid chromatography. Relative abundance is shown in arbitrary units, based on absorbance at 279 nm. The small peak to the right of DDC, at 13.85 min, is a contaminant found in the substrate solution.

- (a) Reaction catalyzed by ObEGS1.
 (b) Reaction catalyzed by PhIGS1.
 (c) Reaction catalyzed by CbIGS1.
 (d) Reaction catalyzed by CbEGS1.
 (e) Reaction catalyzed by CbEGS2.
 (f) Reaction catalyzed by PhEGS1.

by fusing the first 95 codons of *CbEGS1* with codons 96–318 of *CbIGS1*. This hybrid protein catalyzed the formation of mostly eugenol, with a small proportion of isoeugenol (mutant 1 in Table 4). (The reciprocal hybrid protein, which was soluble and stable to a similar degree as the first hybrid protein, did not show any activity.) Since the result suggested that the product specificity mostly resides in region 73–95, site-directed mutagenesis of CbIGS1 was used to change individual residues or a cluster of residues in this region to the corresponding amino acids found in CbEGS1. Changing residues 83, 84, 87, and 88 (mutant 3) gave a protein with the highest ratio of eugenol/isoeugenol production, 85:15. Changing residues 73, 77, 83, and 84 (mutant 2) gave a product with a 29:71 eugenol/isoeugenol ratio. In contrast, changing amino acids at positions 91, 92, and 95 (mutant 4) did not affect the product preference. These data

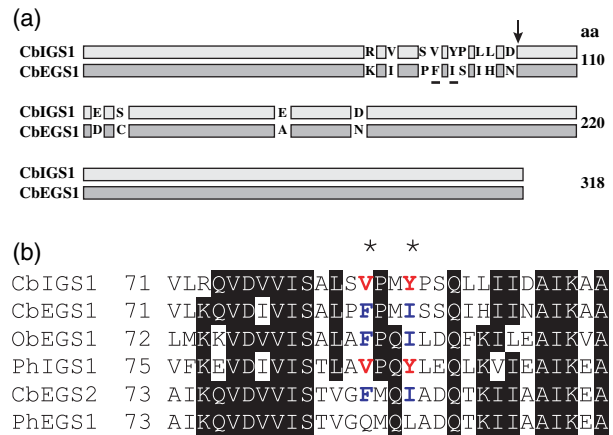


Figure 7. Divergence in eugenol synthase (EGS) and isoeugenol synthase (IGS) sequences.

(a) Schematic representation of differences between CbIGS1 and CbEGS1. Amino acid residues shown to account for significant differences in product specificity are underlined. The position delineating the splice site in the construction of the hybrid proteins is marked with an arrow.

(b) Amino acid sequence alignments of phenylpropane synthases in a segment encompassing the highly divergent region between CbEGS1 and CbIGS1. The positions of the two amino acids found to account for most of the differences in product specificity are marked by asterisks, and the conserved V and Y in IGS enzymes and the conserved F and I in EGS enzymes at these positions are shown by red and blue, respectively.

Table 4 Preferential product formation in eugenol synthase (EGS) and isoeugenol synthase (IGS)

Species	Mutant no.	Mutations (EGS:IGS)	Product proportions
<i>Clarkia</i>	CbIGS1	Wild type	0:100
	1 ^a	R73K, V77I, S83P, V84F, Y87I, P88S, L91I, L92H, D95N	76:24
	2	R73K, V77I, S83P, V84F	29:71
	3	S83P, V84F, Y87I, P88S	85:15
	4	L91I, L92H, D95N	0:100
	5	S83P, V84F	16:84
	6	Y87I, P88S	66:34
	7	V84F, Y87I	75:25
	8	V84F	39:61
	9	Y87I	62:38
	CbEGS1	Wild type	100:0
	10	F84V, I87Y	31:69
	CbEGS2	Wild type	100:0
	11	F86V, I89Y	88:12
Basil	ObEGS1	Wild type	100:0
	12	F85V, I88Y	64:36
<i>Petunia</i>	PhIGS1	Wild type	0:100
	13	V88F, Y91I	39:61
	PhEGS1	Wild type	100:0
	14	Q86V, L89Y	81:19

^aThe hybrid protein, CbEGS1/CbIGS1.

suggested that residues at position 83, 84, 87, and 88, or at least some of them, affect the product forming specificity significantly.

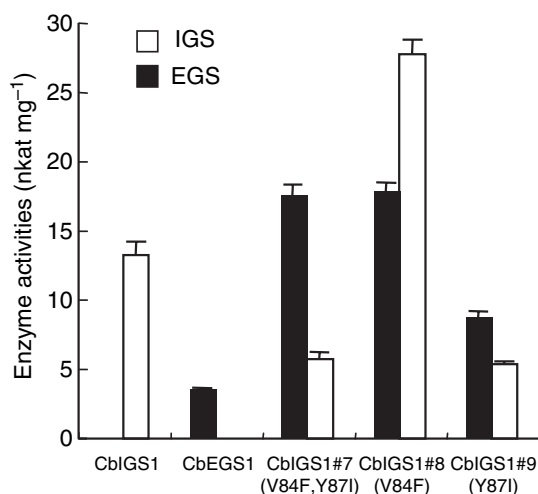


Figure 8. Specific activities of the wild type and *Clarkia breweri* IGS1 mutants. Each value in the figure is an average of three independent experiments. Bars indicate SE.

To narrow down the contribution of these residues to product specificity, five additional mutants were generated (mutants 5–9 in Table 4). Among these mutants, mutant 7, in which residue V84 was changed to F and residue Y87 was changed to I, had the highest ratio of eugenol to isoegenol formation, 75:25, followed by mutant 6 (66:34). Moreover, even the single substitution at position 87 produced a protein which catalyzed the formation of more eugenol than isoegenol (62:38, mutant 9 in Table 4).

Affects of amino acid changes in CbIGS1 on the specific activity of the mutant enzymes

To determine how the amino acid changes described above affected the specific activity of the proteins, we measured this parameter for mutants 7, 8, and 9. Mutants 7 and 8 exhibited 1.8- and 3.4-fold higher total activity, respectively, compared with the wild-type enzyme (Figure 8). In contrast, the change at position 87 (mutant 9, Y87I) had no significant effect on total specific activity of the protein (Figure 8), even though the amino acid at this position appears to contribute most to the product specificity (Table 4).

Site-directed mutagenesis of CbEGS1, ObEGS1, PhIGS1, PhEGS1, and CbEGS2

Since positions 84 and 87 in CbIGS1 were identified as key positions determining product specificity, we examined the specific amino acids in the corresponding positions in the other EGS and IGS proteins identified in this and previous studies (Figure 7b; these positions are numbered slightly differently in each protein because of differences in upstream sequences, but for clarity the numbers referring to

the CbIGS1 positions are used in the text to discuss comparisons). At position 84, both IGS enzymes (CbIGS1 and PhIGS1) have a V, while three EGS enzymes have F and one (PhEGS1) has Q. At position 87, both IGS proteins have Y, while three EGS proteins have I and one (again, PhEGS1) has L. The amino acids in these two positions in each protein were then changed to the corresponding residues in CbIGS1 (for EGS enzymes) or CbEGS1 (for PhIGS1). In each case, some change in product specificity, ranging from 12% to 69%, was observed (Table 4, mutants 10–14).

Discussion

C. breweri and P. hybrida have distinct synthases for eugenol and isoegenol biosynthesis

Purification of EGS and IGS activities from *C. breweri* flowers yielded three distinct proteins, two of which display only EGS activity and the third possessing only IGS activity. One of the *C. breweri* EGSs identified in this approach of direct protein purification and characterization, CbEGS2, proved to be only distantly related to the previously characterized basil EGS and petunia IGS, and its sequence was used to identify a gene from petunia, *PhEGS1*, that encodes a EGS. All three newly characterized *C. breweri* enzymes and the new petunia EGS, as well as the previously characterized PhIGS1 and ObEGS1, use coniferyl acetate to make a single product – either eugenol or isoegenol – and have similar affinity to the substrate, although their catalytic efficiencies may differ by as much as sixfold. The lower catalytic efficiency of PhEGS1 and its lower level of expression compared with PhIGS1 may explain the much lower levels of eugenol, as compared with isoegenol, emitted from petunia flowers.

Few residues in EGS and IGS enzymes have a major effect on product specificity

Our earlier crystallographic studies (Louie *et al.*, 2007) of ObEGS1 in complex with an analog of coniferyl acetate, (7S,8S)-ethyl (7,8-methylene)-dihydroferulate (EMDF), clearly revealed the substrate-binding mode within the ObEGS1 active site (Figure 9a). The guaiacol ring is stacked against the nicotinamide ring of the co-factor, and the side chain, which in EMDF bears a cyclopropyl group and is distinctly kinked, is accommodated in a predominantly hydrophobic pocket at the top of the active-site pocket. Notably, the coniferyl acetate substrate would be most appropriately positioned for acceptance at C7 of a hydride from the cofactor nicotinamide, consistent with the formation of the eugenol product (Figure 9a).

The results from our *in vitro* mutagenesis experiments suggest that the residues at positions 84 and 87 in CbIGS1

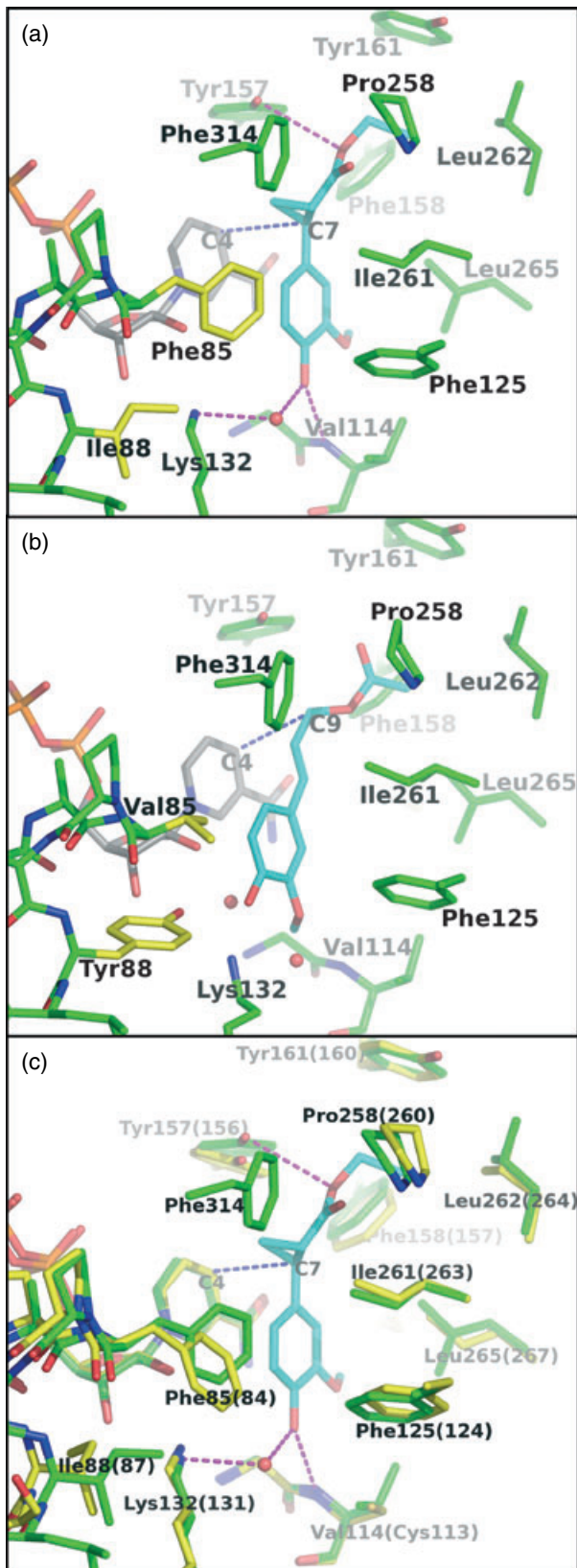


Figure 9. Views of the active sites of ObEGS1, ObEGS1 (F85V, I88Y), and CbEGS1.

(a) ObEGS1 complexed with (7S,8S)-ethyl (7,8-methylene)-dihydroferulate (EMDF; Louie *et al.*, 2007): green, eugenol synthase (EGS) active site residues; yellow, sites of amino acid substitutions; gray, NADP⁺ cofactor; cyan, substrate.

(b) Crystal structure of ObEGS1 (F85V, I88Y) with modeled coniferyl acetate. The binding of the substrate was modeled manually based initially on the observed binding mode of EMDF with wild-type ObEGS1, and adjusted to fill the space vacated by F85 side chain and to form a hydrogen bond between Y88 and the substrate C4-OH. Color coding is as in (a).

(c) Comparison of the active sites of ObEGS1 (green) and CbEGS1 (yellow, residue numbering in parentheses) superimposed. The EMDF is shown from the complex with ObEGS1.

and at the corresponding positions in the other EGS and IGS proteins in this study (Figure 7b) are major determinants of product specificity. Through a protocol identical to that used for the crystallographic analysis of wild-type ObEGS1 (Louie *et al.*, 2007), we have now determined the structure of the ObEGS1 (F85V, I88Y) variant (mutant 12 in Table 4). This structure shows that the Y88 side chain projects into the base of the substrate-binding pocket (Figure 9b). The positioning of the Y88 side chain is assisted by the accompanying replacement of F85 by a residue bearing a smaller side chain, V. The bulky Y ring causes a slight displacement of neighboring residues within the active site, most notably the K132 side chain. The altered positioning of K132, the enlarged space arising from the loss of the bulky F85 side chain, and the introduction of an additional hydrogen bonding group (OH of Y88) that could interact with the C3 or C4 oxygen atoms of the substrate are likely to lead to a shift in the location of the substrate binding site, so that C9 is more appropriately positioned as the hydride acceptor, with the consequence that the altered enzyme produces a significant level (36%) of isoeugenol.

We have also elucidated the structure of the holo-enzyme form of CbEGS1, without additional bound substrate or product analogs. The active sites of CbEGS1 and ObEGS1 are shown to be nearly identical (Figure 9c). Therefore, for these two enzymes, equivalent amino acid replacements would be expected to effect similar outcomes in product specificity, and, in general, this prediction is borne out by the results of the mutagenesis experiments. Nevertheless, in comparison to the ObEGS1 (F85V, I88Y) variant, the corresponding CbEGS1 (F84V, I87Y) variant (mutant 10 in Table 4) produces a much greater proportion of isoeugenol (69% versus 36%). In addition, the reciprocal changes in CbIGS1 (V84F, Y87I) produce more striking effects on product specificity (75% eugenol, mutant 7 in Table 4) than in petunia IGS (39% eugenol). A detailed understanding of the greater effect of these amino acid replacements on *C. breweri* EGS1 and IGS1, which are not apparent through modeling, must await structural analysis of these enzymes in complex with substrate, product(s), or analog.

The observation that changes of just a few residues can lead to new substrate or product specificity is also consistent with what has been found in other families of enzymes involved in specialized metabolism (Pichersky *et al.*, 2006), for example the terpene synthase family, which also consists of several groups of enzymes that, within each group, use the same substrate but produce a different product (and, sometimes, multiple products from this same substrate).

Evolution of enzymatic function in the PIP reductase family

The previously identified petunia PhIGS1 and basil ObEGS1 were shown to be members of the PIP family of reductases, which also includes isoflavone reductase (IFR), pinosresinol-lariciresinol reductase (PLR), phenylcoumaran benzylic ether reductase (PCBER), pterocarpan reductase (PTR), and leucoanthocyanidin reductase (LAR; Figure 3b). Our phylogenetic analyses indicate with high degree of certainty that PhIGS1 and ObEGS1 fall into close but separate clades, and that CbEGS2 and PhEGS1, on the other hand, are closely related to a complex clade that contains proteins biochemically characterized to possess PCBER, IFR, and PTR activities.

The highly similar CbIGS1 and CbEGS1 (96% identity) both fall into the same clade with ObEGS1. The basal position of ObEGS1 in this clade suggests that the ancestor of CbIGS1 and CbEGS1 had EGS activity. However, since no other protein in this clade besides these three proteins has been biochemically characterized, such a conclusion is tentative. However, it is clear that the function of these two proteins diverged recently, and thus the origin of the IGS activity of CbIGS1 evolved independently of PhIGS1 (alternatively, if the ancestral protein in this clade had IGS activity, then the EGS activity of CbEGS1 evolved independently of ObEGS1).

Surprisingly, the CbEGS2 and PhEGS1 proteins fall in a clade in which proteins characterized to have PCBER activity as well as IFR and PTR enzymes also reside (Figure 3b). In this clade, the branching of IFR enzymes and the single PTR enzyme currently known, all from legumes, is uncertain: in the neighbor-joining tree the position of these two branches is reversed relative to each other, and in the maximum parsimony tree (legend to Figure 3b), all of these four sequences are monophyletic. However, in all of these trees the gymnospermous PCBER sequences (PtdPCBER from *P. taeda* and ThPCBER from *Thuja plicata*) constitute an outgroup to the IFRs, PTR, the angiospermous PCBER sequences (PtPCBER from *P. trichocarpa* and FiPCBER from *Forsythia intermedia*), and CbEGS2 and PhEGS1.

Gang *et al.* (1999), in their original report on the characterization of PCBER enzymes, pointed out that the *P. taeda* and *P. trichocarpa* PCBER enzymes (the only PCBER enzymes for which V_{\max} values have been reported) have an extremely low turnover rate with DDC that 'cannot be

explained at the present time'. They showed that they could not reduce pinosresinol, but, understandably, they did not test these enzymes with coniferyl acetate as EGS and IGS and their substrate were not known at the time. We show here that CbEGS2 and PhEGS1 also have very low turnover rates for the reduction of DDC that are comparable with that of *P. trichocarpa* and *P. taeda* PCBER enzymes. On the other hand, CbEGS2 and PhEGS1 each have a turnover rate for coniferyl acetate that is several thousand-fold higher than their rates with DDC and similar to the turnover rates of CbEGS1, CbIGS1, ObEGS1 and PhIGS1 with coniferyl acetate. These results indicate that CbEGS2 and PhEGS1 are *bona fide* EGSs, and further suggest that the sequences currently characterized as PCBER enzymes, as well as other sequences in this branch, might in fact prefer coniferyl acetate or other related substrates to DDC. While we were writing this paper, Vassão *et al.* (2007) reported that a PCBER-related protein (despite their title, the protein investigated was more similar to PCBER than to PLR) in the creosote bush (*Larrea tridentate*) is capable of synthesizing phenylpropenes from esters of alcohols of lignin precursors. However, this activity was not linked to specific phenylpropenes in the plant, nor was the PCBER activity of this protein examined.

Whether the ancestral protein of this clade was a *bona fide* EGS that used coniferyl acetate or another type of enzyme, and what the biochemical activities of the many other uncharacterized proteins in this clade are (deduced from ESTs and representing a wide variety of plant species) remain intriguing questions that will require additional studies to resolve. However, the phylogenetic analysis suggests that the protein that was ancestral to this clade as well as to the LAR and PLR clades was unlikely to be an EGS/IGS. It thus appears likely that phenylpropene synthases have evolved independently at least twice during plant evolution. A less likely scenario is that the ancestor of the entire family possessed phenylpropene synthase activity, in which case it appears that the phenylpropene synthases eventually evolved for unknown reasons into two distinct lineages.

Koeduka *et al.* (2006) have presented indirect evidence that ObEGS1 and PhIGS1 use a quinone methide intermediate-based mechanism to generate an intermediate to which the reductive transfer of the reducing hydride can then be easily accomplished, and Akashi *et al.* (2006) have proposed that some other PIP enzymes may also use the same mechanism on substrates that, like coniferyl acetate, contain a *para*-hydroxybenzyl moiety. The recent structure-function studies utilizing the crystal structure of basil EGS indeed support this hypothesis (Louie *et al.*, 2007). Thus, the potential to generate a quinone-methide intermediate with a variety of substrates that share a *para*-hydroxybenzyl moiety appears to underlie the basis for the multiple types of substrates that the PIP family enzymes have evolved to

handle. In addition to the previously demonstrated diversity of the PIP family, we now show here that the same product specificity, and most likely the same substrate specificity, have evolved independently more than once. Overall, these results highlight the strong potential for the evolution of new functions inherent in this family.

Experimental procedures

Plant materials and growth condition

Clarkia breweri were grown as described in Raguso and Pichersky (1995). *Petunia hybrida* cv. Mitchell (Ball Seed, <http://www.ballseed.com/>) plants were grown in the greenhouse with a 16-h light period (supplemented to 100 $\mu\text{mol m}^{-2} \text{sec}^{-1}$) and temperature of 21°C, and an 8-h dark period at 16°C.

Chemicals and substrates

Chemicals were from Sigma-Aldrich (<http://www.sigmaaldrich.com/>) unless noted. Coniferyl acetate was synthesized as previously described (Koeduka et al., 2006). Dehydroconiferyl alcohol was synthesized and verified according to Gang et al. (1999).

Enzyme assays

The EGS and IGS enzymatic reactions were performed and products were analyzed as previously described (Koeduka et al., 2006), except that a temperature gradient from 50°C to 275°C at 14°C min⁻¹ was applied during gas chromatography/mass spectrometry (GC-MS). For PCBER enzymatic assays, we used identical conditions to the one employed for EGS/IGS assays, except that the substrate DDC was used instead of coniferyl acetate. The product of the reaction was identified by the published retention value (Gang et al., 1999) and by its UV absorption spectrum.

Protein purification

All manipulations were carried out at 4°C unless stated otherwise. Crude extract (50 ml, representing 5.0 g fresh weight petal tissue) was loaded onto a DEAE-cellulose column (8 ml of DE53, Whatman, <http://www.whatman.com/>) that was pre-equilibrated with a solution containing 25 mM Bis-2-amino-2-(hydroxymethyl)-1,3-propanediol (Bis-Tris), pH 7.0, and 1 mM DTT (buffer A). After a wash with 20 ml of buffer A, IGS and EGS activities were eluted with 20 ml of buffer A containing 200 mM KCl. Fractions with the highest IGS and EGS activities (which co-eluted) were pooled and loaded on a Hitrap-Phenyl HP column (0.7 × 2.5 cm, Pharmacia Biotech Inc.; <http://www.gehealthcare.com>) pre-equilibrated with 1 M (NH₃)₂SO₄ in buffer A at a flow rate of 0.5 ml min⁻¹. After washing with 5 ml of 1 M (NH₃)₂SO₄ in buffer A, the activities were eluted with a linear reverse gradient (15 ml) from 1 M (NH₃)₂SO₄ in buffer A to 0 M (NH₃)₂SO₄ in buffer A followed by an additional 15 ml of buffer A. Fractions containing peak IGS activity and the first peak of EGS activity (which co-eluted) were pooled (total 6.75 ml) and loaded onto Hitrap-Q HP column (0.7 × 2.5 cm; Pharmacia Biotech Inc.) previously equilibrated with buffer A, followed by a wash with 5 ml of buffer A and then IGS and EGS activities were eluted with 20 ml linear gradient (0–400 mM) of KCl in buffer A at flow rate of 0.5 ml min⁻¹. Fractions containing the second peak of EGS activity

from the Hitrap-Phenyl HP column were pooled and similarly loaded onto a second Hitrap-Q HP column and the column treated similarly.

Protein sequencing

The 36-kDa protein band (Figure 2, lane 1) was eluted from the gel, trypsinized, and subjected to LC-MS/MS analysis as previously described (Chen et al., 2005), followed by a search of the *C. breweri* flower EST database using the program MASCOT (Perkins et al., 1999). Seven unique peptides obtained from this 36-kDa protein band (RSMGVTHIEGEMEEHEKM, KFVLNVEEDIAKY, RIVYRPPKN, KSLGSLFKK, KVHMPDEQLVRL, RLSQELPQPONIPVLSILHSIFVKG, RKDDIEASNLYPELEFSTIDGLLDLFIISGRA) matched the two closely related protein sequences encoded by *CbEGS1* and *CbIGS1* (see Results) at a significance threshold of 0.001. At this stringency no peptide hits were found in a randomized database of the same size and amino acid composition, suggesting a very low false positive rate. The single protein of approximate molecular mass 38 kDa in the peak EGS activity eluting from the second Hitrap-Q column (Figure 2, lane 2) was analyzed in the same way, and 11 peptide sequences were obtained from it (KILIIIGGTGYIGKF, KFIVEASVKE, KEGHPTFALVRE, RETTVSDPVKGL, KFNGLVSLLYGDLYDHDLSL-VKA, KQVDVVISTVGFMIADQTKI, KIIAAIKE, KEAGNVKRF, KRFF-PSEFGNDVDHVNAVEPAKS, KSVAFVKA, RDKVIIPGDGNPKA) matched the protein sequence encoded by *CbEGS2* (Figure 3a).

Quantitative RT-PCR

Total RNA was isolated from *C. breweri* as previously described (Dudareva et al., 1996) and from *petunia* as described by Boatright et al. (2004). For quantitative (q)RT-PCR, first-strand cDNA synthesis and qPCR reactions with gene-specific primers (Table S1) were performed as previously described (Varbanova et al., 2007).

Isolation, characterization, and expression in *E. coli* of *C. breweri* cDNAs encoding proteins with IGS and EGS activities

As described in Results, a 5' RACE experiment (Chenchik et al., 1996; Matz et al., 1999) was performed, using internal primers (Table S1), to obtain the complete sequence of *CbIGS1*. To construct *E. coli* expression vectors, full-length cDNAs were amplified by RT-PCR from flower RNA with forward and reverse primers (Table S1), the PCR fragments were spliced into pENTR (Invitrogen, <http://www.invitrogen.com/>), and analyzed by sequencing and the cDNA fragment was transferred to the expression vector pHis9, a modified pET/T7 vector (Varbanova et al., 2007), to give an N-terminal in-frame addition of a peptide containing nine His residues. Expression in *E. coli* (BL21-CodonPlus-RIL) and DEAE and His-tag affinity purification of the proteins were performed as previously described (Koeduka et al., 2006; Nishimoto et al., 2007). *CbEGS1*, *CbIGS1*, and *CbEGS2* were also amplified and spliced directly into the *E. coli* expression vector pEXP5-CT/TOPO (Invitrogen) for production of non-fused, non-tagged proteins.

In vitro mutagenesis

The EGS and IGS mutants were constructed in the pEXP5-CT/TOPO TA expression vector (Invitrogen) with the PCR method (Ho et al., 1989). The mutagenic primers for each mutation were designed in complementary pairs (Table S1). Mutations were confirmed by sequencing both strands.

Structural studies

Crystals of the ObEGS1 (F85V, I88Y) variant were obtained using the same protocol previously employed for wild-type ObEGS1 (Louie *et al.*, 2007). Determination of the structure of the ObEGS1 variant was initiated with the isomorphous, orthorhombic crystal structure of wild-type ObEGS1 (Protein Data Bank entry 2QX7), and yielded a refined atomic model at a resolution of 2.15 Å with a crystallographic *R*-factor of 0.255 (free *R* 0.287). Crystals of CbEGS1 were grown from solutions of the protein mixed with 0.1 M sodium citrate (pH 5.4), 20% (v/v) isopropanol, 20% (w/v) polyethylene glycol 4000, and 5 mM NADP⁺. These crystals belong to space group C2 with unit-cell parameters *a* = 67.3 Å, *b* = 87.4 Å, *c* = 51.5 Å, and β = 101.3. The initial structure solution of CbEGS1 was obtained by molecular replacement with a homology model constructed from ObEGS1. The atomic model of CbEGS1 was refined against X-ray data to 1.8-Å resolution with a crystallographic *R*-factor of 0.188 (free *R* 0.217). All crystallographic procedures employed were as described previously (Louie *et al.*, 2007). X-ray diffraction data were measured at beamline 8.2.2 of the Advanced Light Source (Lawrence Berkeley National Laboratory). The atomic coordinates and structure factors were deposited in the PDB under accession codes 3C3X [ObEGS1 (F85V, I88Y)] and 3C1O (wild-type CbEGS1).

Phylogenetic analyses

Multiple alignments of 32 PIP protein sequences were constructed using the MUSCLE (Edgar, 2004) program. Alignment columns containing more than 16 gap characters were removed prior to tree reconstruction. Sequence distance matrix was constructed using the PROTDIST program of the PHYLIP package (Felsenstein, 1996) with the Jones–Taylor–Thornton evolutionary model (Jones *et al.*, 1992). Neighbor-joining and least-squares trees were constructed using the NEIGHBOR and FITCH programs, respectively, of the PHYLIP package. The maximum parsimony tree was constructed using the PROTPARS program of the PHYLIP package. The maximum likelihood tree was constructed using the PROTML program of the MOLPHY package (Hasegawa *et al.*, 1991) by optimizing the least-squares tree with local rearrangements (Jones–Taylor–Thornton evolutionary model with adjustment for observed amino acid frequencies). Reliability of the internal branches was estimated using 10 000 resampling of the estimated log likelihood (RELL) bootstrap replications using the PROTML program of the MOLPHY package.

Acknowledgements

We thank Dr Yuri I. Wolf (Associate Investigator, NCBI/NLM/NIH) for performing the phylogenetic analyses. This work was supported by National Science Foundation grants 0331353, 0312466, and 0718152 to EP, by National Science Foundation grant 0718064 to JNP, by National Research Initiative of the US Department of Agriculture Cooperative State Research, Education, and Extension Service grant 2005-35318-16207 and National Science Foundation/USDA-NRI Interagency Metabolic Engineering Program grant 0331333 to ND, and by a grant from the Fred Gloeckner Foundation, Inc to ND. JPN is an investigator of the Howard Hughes Medical Institute.

Supplementary Material

The following supplementary material is available for this article online:

Table S1. Primer sequences used in this study.

Table S2. Accession numbers of sequences from Figure 3.

This material is available as part of the online article from <http://www.blackwell-synergy.com>

Please note: Blackwell publishing are not responsible for the content or functionality of any supplementary materials supplied by the authors. Any queries (other than missing material) should be directed to the corresponding author for the article.

References

- Akashi, T., Koshimizu, S., Aoki, T. and Ayabe, S. (2006) Identification of cDNAs encoding pterocarpan reductase involved in isoflavan phytoalexin biosynthesis in *Lotus japonicus* by EST mining. *FEBS Lett.* **580**, 5666–5670.
- Boatright, J., Negre, F., Chen, X. *et al.* (2004) Understanding *in vivo* benzenoid metabolism in petunia petal tissue. *Plant Physiol.* **135**, 1993–2011.
- Chen, H., Wilkerson, C.G., Kuchar, J.A., Phinney, B.S. and Howe, G.A. (2005) Jasmonate-inducible plant enzymes degrade essential amino acids in the herbivore midgut. *Proc. Natl Acad. Sci. USA*, **102**, 19237–19242.
- Chenchi, A., Zhu, Y., Diatchenko, L., Li, A., Hill, J. and Siebert, P. (1996) Generation and use of high-quality cDNA from small amounts of total RNA by SMART PCR. In *RT-PCR Methods for Gene Cloning and Analysis* (Siebert, P. and Larrick, J., eds). Westborough, MA: BioTechniques Books, pp. 305–319.
- D'Auria, J.C., Chen, F. and Pichersky, E. (2002) Characterization of an acyltransferase capable of synthesizing benzyloxyacetate and other volatile esters in flowers and damaged leaves of *Clarkia breweri*. *Plant Physiol.* **130**, 466–476.
- Dudareva, N., Cseke, L., Blanc, V.M. and Pichersky, E. (1996) Evolution of floral scent in *Clarkia*: novel patterns of *S*-linalool synthase gene expression in the *C. breweri* flower. *Plant Cell*, **8**, 1137–1148.
- Edgar, R.C. (2004) MUSCLE: multiple sequence alignment with high accuracy and high throughput. *Nucleic Acids Res.* **32**, 1792–1797.
- Felsenstein, J. (1996) Inferring phylogenies from protein sequences by parsimony, distance, and likelihood methods. *Methods Enzymol.* **266**, 418–427.
- Gang, D.R., Wang, J., Dudareva, N., Nam, K.H., Simon, J.E., Lewinsohn, E. and Pichersky, E. (1999) Evolution of plant defense mechanisms. Relationships of phenylcoumaran benzylic ether reductases to pinoresinol–lariciresinol and isoflavone reductases. *J. Biol. Chem.* **274**, 7516–7527.
- Gang, D.R., Wang, J., Dudareva, N. *et al.* (2001) An investigation of the storage and biosynthesis of phenylpropenes in sweet basil. *Plant Physiol.* **125**, 539–555.
- Grossman, J. (1993) Botanical pesticides in Africa. *Int. Pest. Manag. Pract.* **15**, 1–9.
- Hasegawa, M., Kishino, H. and Saitou, N. (1991) On the maximum likelihood method in molecular phylogenetics. *J. Mol. Evol.* **32**, 443–445.
- Ho, S.N., Hunt, H.D., Horton, R.M., Pullen, J.K. and Pease, L.R. (1989) Site-directed mutagenesis by overlap extension using the polymerase chain reaction. *Gene*, **77**, 51–59.
- Jones, T., Taylor, W.R. and Thornton, J.M. (1992) The rapid generation of mutation data matrices from protein sequences. *CABIOS*, **8**, 275–282.
- Koeduka, T., Fridman, E., Gang, D.R. *et al.* (2006) Eugenol and isoeugenol, characteristic aromatic constituents of spices, are biosynthesized via reduction of coniferyl alcohol esters. *Proc. Natl Acad. Sci. USA*, **103**, 10128–10133.
- Louie, G.V., Baiga, T.J., Bowman, M.E., Koeduka, T., Taylor, J.H., Spassova, S.M., Pichersky, E. and Noel, J.P. (2007) Structure and

- reaction mechanism of basil eugenol synthase. *PLoS ONE*, **2**, e993.
- Matz, M., Lukyanov, S., Bogdanova, E., Britanova, O., Lukyanov, S., Diatchenko, L. and Chenchik, A.** (1999) Amplification of cDNA ends based on template-switching effect and step-out PCR. *Nucleic Acids Res.* **27**, 1558–1560.
- Min, T., Kasahara, H., Bedgar, D.L. et al.** (2003) Crystal structures of pinoreosinol-lariciresinol and phenylcoumaran benzylic ether reductases and their relationship to isoflavone reductases. *J. Biol. Chem.* **278**, 50714–50723.
- Nishimoto, M., Fushinobu, S., Miyanaga, A., Kitaoka, M. and Hayashi, K.** (2007) Molecular anatomy of the alkaliphilic xylanase from *Bacillus halodurans* C-125. *J. Biochem.* **5**, 709–717.
- Obeng-Ofori, D. and Reichmuth, C.** (1997) Bioactivity of eugenol, a major component of essential oil of *Ocimum suave* (Wild.) against four species of stored-product Coleoptera. *Int. J. Pest. Manage.* **43**, 89–94.
- Perkins, D.N., Pappin, D.J., Creasy, D.M. and Cottrell, J.S.** (1999) Probability-based protein identification by searching sequence databases using mass spectrometry data. *Electrophoresis*, **20**, 3551–3567.
- Pichersky, E., Raguso, R.A., Lewinsohn, E. and Croteau, R.** (1994) Floral scent production in *Clarkia* (Onagraceae) I. Localization and developmental modulation of monoterpene emission and linalool synthase activity. *Plant Physiol.* **106**, 1533–1540.
- Pichersky, E., Noel, J.P. and Dudareva, N.** (2006) Biosynthesis of plant volatiles: nature's diversity and ingenuity. *Science*, **311**, 808–811.
- Prasad, N.S., Raghavendra, R., Lokesh, B.R. and Naidu, K.A.** (2004) Spice phenolics inhibit human PMNL 5-lipoxygenase. *Prostaglandins Leukot. Essent. Fatty Acids*, **70**, 521–528.
- Raguso, R.A. and Pichersky, E.** (1995) Floral volatiles from *Clarkia breweri* and *C. concinna* (Onagraceae): recent evolution of floral scent and moth pollination. *Plant Syst. Evol.* **194**, 55–67.
- Tanner, G.J., Francki, K.T., Abrahams, S., Watson, J.M., Larkin, P.J. and Ashton, A.R.** (2003) Proanthocyanidin biosynthesis in plants. Purification of legume leucoanthocyanidin reductase and molecular cloning of its cDNA. *J. Biol. Chem.* **278**, 31647–31656.
- Varbanova, M., Yamaguchi, S., Yang, Y. et al.** (2007) Methylation of gibberellins by *Arabidopsis* GAMT1 and GAMT2. *Plant Cell*, **19**, 32–45.
- Vassão, D.G., Kim, S.J., Milhollan, J.K., Eichinger, D., Davin, L.B. and Lewis, N.G.** (2007) A pinoreosinol-lariciresinol reductase homologue from the creosote bush (*Larrea tridentata*) catalyzes the efficient in vitro conversion of p-coumaryl/coniferyl alcohol esters into the allylphenols chavicol/eugenol, but not the propenylphenols p-anol/isoegenol. *Arch. Biochem. Biophys.* **465**, 209–218.
- Verdonk, J.C., Ric de Vos, C.H., Verhoeven, H.A., Haring, M.A., van Tunen, A.J. and Schuurink, R.C.** (2003) Regulation of floral scent production in petunia revealed by targeted metabolomics. *Phytochemistry*, **62**, 997–1008.
- Wang, J., Dudareva, N., Bhakta, S., Raguso, R.A. and Pichersky, E.** (1997) Floral scent production in *Clarkia breweri* (Onagraceae). II. Localization and developmental modulation of the enzyme S-adenosyl-L-methionine:(iso)eugenol O-methyltransferase and phenylpropanoid emission. *Plant Physiol.* **114**, 213–221.